Numerical Study of Partially Premixed Combustion in a Iso-Octane Flame

C. Jiménez [1,*], B. Cuenot[1] and T. Poinsot [1,2]

December 3, 2001

1. CERFACS. France.

2. IMFT. France. * Present affiliation: LITEC-CSIC. Spain.

Colloquium: Turbulent combustion Keywords: Partially Premixed Combustion

Word count: approx. 2900 w + 2eq *21 + 1eq *42 + 1 table*400 + 4 figures *400 = 4963

Corresponding author:

C. Jiménez • LITEC-CSIC • María de Luna 10 • 50015 Zaragoza. Spain. •

Tel 34 976 71 63 03. • Fax 34 976 76 18 82. • email: carmela@litec.csic.es

Abstract

Numerical simulations of stratified combustion of an iso–octane / air mixture are used to study the influence of stratification on combustion efficiency and to validate flamelet models for partially premixed combustion. Effects in combustion efficiency are found to be quite significant. In the most favorable stratified case the heat release is increased by 280% compared to the homogeneous combustion with the same amount of fuel and air. These high differences allow a detailed study of the local behavior and structure of the flame, with strong implications for partially premixed combustion modelling.

Introduction

In direct-injection engines, liquid fuel is injected directly into the combustion chamber to generate a highly stratified fuel / air mixture at ignition time. This has the potential to significantly reduce fuel consumption, especially at low–speed light–load operation [1], and has been the subject of intense research for both spark–ignition [2] and compression–ignition Diesel [3] engines. This flame propagating into a non–homogeneous mixture is an example of partially premixed combustion, that is, a situation where the reactants are not perfectly mixed nor completely separated before combustion and for which modeling can not be based on the traditional premixed / non-premixed scenarios. Another example can be found in modern aircraft gas–turbine engines [4], in which fuel and secondary air are injected at various locations, resulting in a non-uniform equivalence ratio at the flame front.

Research in the field of partially premixed combustion has shown contradictory results concerning the efficiency of combustion in non-homogeneous conditions as compared to a uniformly premixed case with the same amount of fuel and air. While the experimental measurements of Zhou et al. [5] imply that the wrinkling effect dominates and overall burning rates are higher in non-homogeneous reactants for a broad range of global stoichiometries and degrees of partial premixing, many of the earlier simulations found no effect or an opposite effect [6, 7, 8]. More recent simulations have shown that several competing effects determine whether the global burning rate is enhanced or reduced as a result of partial premixing. For example the flame front area is expected to be higher in non-homogeneous reactants because of wrinkling induced by different propagating speeds in rich/lean pockets, and the mean flame speed $< S_L >$ can be higher or lower depending on the distribution of reactant equivalence ratio [9]. Depending on the distribution of non-homogeneous pockets in equivalence ratio space and physical space, burning rates in propane / air partially premixed systems could be up to 50 % higher than in homogeneous mixtures.

As a continuation of the mentioned works, this study presents numerical simulations of combustion in perfectly premixed and partially premixed (stratified) mixtures of iso–octane / air, more relevant to engine studies, in conditions otherwise similar to those of [9]. Results are used to investigate the flame response to variable equivalence ratio and the resulting local flame structure.

Description of the simulations

The approach adopted is to perform direct numerical simulations (DNS) of a premixed flame propagating into perfectly premixed and partially premixed iso–octane / air mixtures. The system considered is a compressible multi–component ideal–gas mixture, for which the conservation equations for mass, momentum, chemical species mass fractions and total energy are solved using the NTMIX–CHEMKIN code [10] in a two–dimensional rectangular domain. High–order space and time integration of the equations is performed using sixth–order compact finite–differences [11] and a third–order Runge–Kutta temporal scheme. A detailed reaction mechanism for iso–octane based on 26 species and 40 reactions chemistry [12], multicomponent molecular transport of species and full resolution of both the turbulent and the chemical scales allow reliable simulations. The elementary reaction production terms and multicomponent molecular transport coefficients are computed using the CHEMKIN and TRANSPORT packages [13, 14]. In the perfectly premixed simulation a steady laminar flame separates initially reactants from products as shown in Fig.1. Isotropic two–dimensional turbulence is superimposed to the laminar flame using a prescribed turbulence energy spectrum with imposed rms turbulent velocity u_{To} and integral length scale l_{T0} [15]. Other parameters are the initial turbulent Reynolds number $Re_{T0} = u'_{T0} l_{T0}/\nu_u$, the initial laminar flame propagation speed S_L^0, the initial laminar flame thickness δ_l^0 and the flame time τ_f, defined in [8] as: $\tau_f = 2\delta_l^0/(S_L^0(1 + \rho_u/\rho_b))$. Table 1 reports their values in the present simulations. Aero-thermo-chemical conditions approach those in an automotive gasoline direct-injection engine at low–speed light–load operating conditions (except for the value of l_{T0}, which is lower by an order of magnitude compared to typical engine values [15]). Partial premixing is introduced by varying the initial mass fractions of iso–octane, oxygen and nitrogen, through a periodic perturbation that conserves the total quantity of fuel and oxidizer and the O2 to N2 ratio. All simulations are started with the same homogeneous lean flame, with a transition zone to the non-homogeneous mixture for cases NH1 and NH4. A perturbation scale is defined as $l_{\phi 0} = L_y/n$ where L_y is the length of the domain in y-direction (normal to the flame propagation) and n the number of periods of the perturbation across L_y. Three different distributions of reactant mixtures about the mean were explored; these are compiled in Table 1. Initial conditions in case H are those of a homogeneous lean ($\phi = .6$) mixture; this is used as a reference for the study of stratified cases. Configuration NH1 was designed with asymmetrical non-homogeneities about the mean value $\phi = .6$, as in [9]. This asymmetrical perturbation is closer to conditions in an engine, where fuel is injected as a liquid, leading to a range of [0:2] for ϕ. The relatively higher proportion of fuel that burns at equivalence ratios corresponding to the maximum $S_L(\phi)$ is expected to yield higher heat release per unit flame area for NH1, as was the case in previous propane simulations [9]. Finally, case NH4 presents the same mixture distribution in equivalence ratio space as case NH1 (see Table 1), but a different spatial distribution (smaller length scales, see Fig.1). The initial turbulent field is the same for all cases. Comparison of cases NH1 and NH4 is used to study the effect of spatial distribution of mixture strength on heat release.

Length scales for simulation NH1 and NH4 are selected according to an "effectiveness" criterion as defined in [9]: in case NH1 mixing time is long compared to the flame advancement time and inhomogeneous pockets produce a strong wrinkling of the flame front, while in case NH4 fast mixing effects dominate and inhomogeneities are smoothed before they reach the flame.

The flame thickness for the present thermochemical conditions is of the order of 0.16 mm. The mesh spacing being a small fraction of that ($\Delta x \leq .016mm$), a three–dimensional simulation in a domain that extends over several turbulence integral scales (of the order of several millimeters), would demand CPU times of the order of years.

For the present two–dimensional simulations CPU time requirements are only of the order of two–to–three days on a NEC SX-5 computer. Implications of two–dimensionality have been discussed at length by Haworth and Poinsot [15]. In the case of premixed turbulent flames, the local flame structure is essentially two–dimensional; no fundamentally different results have been reported to date for three– versus two–dimensional numerical simulations. In the case of non-premixed combustion, the implications of two–dimensionality may be more restrictive.

Results

Effects of stratification in combustion efficiency

The heat release rate fields corresponding to time $t/\tau_f = 4$ obtained in the three simulations are shown in Fig.1 (bottom). Also shown are the stoichiometric contour line of the mixture fraction of C and H atoms $Z = z_{C+H}$ and contours of the progress variable c, defined as:

$$Z = z_{C+H} = \sum_{n=1}^{Nspecies} (Y_C^n + Y_H^n), \qquad c = 1 - Y_{C8H18}/z_{C+H} \tag{1}$$

Here Y_C^n and Y_H^n stand for the mass fractions of elements C and H contained in Y^n.

Contours of c mark the flame front, which appears clearly deformed in NH1 as compared to the flame front shape of flame H, due to wrinkling induced by locally varying flame burning speeds. The flame front is only slightly deformed in simulation NH4, as anticipated in the previous section, due to the smaller size of the rich/lean pockets.

The effect of the distribution of reactant mixture can be quantified by comparing magnitudes measured in simulations H, NH1 and NH4. Figure 2 presents the total heat release rate and the flame length as obtained in DNS for the three cases. The total heat release is the summation of the local heat release over the whole computational domain, and is normalized by the total heat release of the initial planar laminar lean ($\phi = .6$) flame. The flame length is computed as the length of a progress variable iso–contour ($c = 0.9$). Time is normalized by the flame time τ_f.

All three flames present a similar initial increase in flame length up to time $t/\tau_f = 2$, reaching there approximately three times the initial length. This similar evolution suggests that turbulent wrinkling dominates at this stage. The transition zone between the initial lean flame and the inhomogeneities is crossed after $t/\tau_f \approx 1$: before this time, no particular effect of partial premixing is expected.

Later, small differences appear, with the non–homogeneous large scale case NH1 showing a faster increase than the homogeneous one and the NH4 case showing a slightly slower increase. Effects of partial premixing in the flame front length are nevertheless very small and the three flames present similar lengths.

The increase rate of the overall heat release is initially smaller than that of the flame length, and by time $t/\tau_f = 2$ it has only reached 1.5 times its initial value in the homogeneous (H) and stratified small scale (NH4) cases, and 2.3 times in the stratifed large scale case NH1. Effects of stratification become significant after this time, with heat release in flame NH1 increasing much more rapidly than in the other two cases. Since the differences in flame length remain comparatively small this different behavior must be related to a locally greater heat release per unit flame length. To better understand this behavior, one-dimensional stationary flames at P=4 atm and T=700 K with different equivalence ratios were computed using PREMIX (a CHEMKIN [13] application) with the same chemical mechanism. A variable equivalence ratio flamelet library was constructed containing the laminar flame speed values for the burning of mixtures of different Z (or equivalence ratio) $S_L(Z)$ and the integrated fuel reaction rate for every flamelet $W_L^F(Z) = \int \dot{\omega}^F(x)dx$. Figure

3 (bottom left) shows the curve $S_L(Z)$ obtained from the flamelet library, normalized by the flame speed $S_L(< Z >) = 48cm/s$ corresponding to the mean mixture fraction $< Z >= 0.037$ ($\phi = .6$), and the distribution (i.e. probability density function) $pdf(Z)$ along the flame interface for cases NH1 and NH4 at two different times. The values of $< S_L(Z) >_\Sigma = \int S_L(Z) pdf(Z) dZ$ measured in the DNS (where $<>_\Sigma$ corresponds to the mean along the flame surface Σ) for cases NH1 and NH4 and times 3 and 4 are also indicated. The average flame speed $< S_L(Z) >_\Sigma$ is increased by a Z-distribution around the mean that favorises the higher values of S_L, i.e. the range $.04 < Z < .11$. In case NH1 it appears that the distribution is well extended towards values corresponding to high flame speeds, whereas in case NH4 the Z-distribution rapidly goes back to a narrow peak around the mean, explaining the different behaviors of the two flames.

The same analysis can be made for the total laminar fuel consumption rate $W_L^F(Z)$ (normalized by $W_L^F(< Z >)$), also obtained from the flamelet library (Fig.3 bottom right). The relation between the laminar flame speed $S_L(Z)$ and the total fuel consumption rate $W_L^F(Z)$ is well defined in the case of one-dimensional premixed flames:

$$S_L(Z) = W_L^F(Z)/(\rho^u Y_F^u(Z)) \tag{2}$$

where the superscript u refers to the unburnt gases. As the fuel mass fraction in the unburnt gases increases with Z, the two curves $S_L(Z)$ and $W_L^F(Z)$ are not proportional. Therefore the increase of the mean flame speed $< S_L(Z) >_\Sigma$ and the increase of the mean total fuel consumption rate $< W_L^F(Z) >_\Sigma$ are not equivalent.

This has a strong implication for flamelet models. These use either the laminar flame speed or the total laminar fuel consumption rate to estimate the total consumption rate of the whole turbulent flame, through a wrinkling factor Σ/Σ^0 where Σ^0 is the initial flame surface. In homogeneous cases, the mixture fraction Z is a constant and the two formulations based on the laminar flame speed or on the total laminar fuel consumption rate are mathematically equivalent. In partially premixed flames this is not the case anymore, due to the following inequality:

$$< S_L(Z) >_\Sigma = \left\langle \frac{W_L^F(Z)}{\rho^u Y_F^u(Z)} \right\rangle_\Sigma \neq \frac{< W_L^F(Z) >_\Sigma}{< \rho^u Y_F^u(Z) >_\Sigma} \tag{3}$$

As a consequence, only one of the above formulations holds in partially premixed flames and further study is needed to answer this question.

As was the case in [9], the stratified case NH1 presents a clear gain in heat release as compared to the homogeneous case H. The efficiency gain in the present simulations reaches values up to 280 %, to be compared with the 50 % gain obtained in the propane simulations of [9], where all conditions were in other respects similar to the present computations.
As the flame of case NH4 does not show significant deviations from the homogeneous flame H, it will not be used for the local analysis of the next section.

Local analysis

Local analysis can be used to further explore the turbulent partially premixed flame as compared to laminar flamelets. In simple one-step chemistry, the fuel reaction rate $\dot{\omega}^F$ is a function of Z and c only. Although this relationship is not exactly true in complex chemistry, it is interesting to study the flame in the $(\dot{\omega}^F, Z, c)$ space for a local analysis.
Figure 4 presents the comparison of the local fuel consumption rate as a function of the local composition (Z, c) for the one-dimensional laminar flamelets library and for the two cases H and NH1 at an intermediate time $t/\tau_f = 3$. The scatter plots correspond to points in the DNS at a given mixture fraction value Z, while lines represent the 1D profiles of premixed laminar flamelets at the same mixture fraction.

Typical deviations of a turbulent flame from a flamelet behavior can be seen in the plot corresponding to case H (right–bottom plot in Fig.4), with points in the turbulent flame located around the flamelet line. Deviations from the flamelet line in the partially premixed case seem to be shifted: locally richer zones (top–left and bottom–left plots) present a local consumption rate smaller than the flamelet, while locally leaner zones present a shift towards higher consumption rates. This could be explained by local burning temperatures and gas compositions different from the flamelet, as a result of transverse mixing between rich and lean zones. In that case, the local temperature at a rich mixture burning zone would be slightly smaller than that of the corresponding flamelet, while the local temperature of a lean zone would be higher. This, combined to different species concentrations, is a clue of the behavior of the partially premixed flame as different to a superposition of different equivalence ratio perfectly premixed flames and has an important impact on the final products concentrations.

Conclusions

Simulations of combustion in a stratified premixed iso-octane/air mixture have been performed under global lean conditions, approaching those of a gasoline direct injection (GDI) engine.

Substantial differences in the amount of heat release between homogeneous and non–homogeneous reactants have been obtained. A strong influence of the mixture distribution in terms of equivalence ratio was found, and it was shown that an appropriate distribution can lead to efficiency gains of about 280 %. The spatial distribution of the inhomogeneities is also an important factor, as it determines the induced flame wrinkling. It was shown that variations in length scales could bring the stratified flame to a behavior close to that of the homogeneous flame, due to the strong turbulent mixing prior to combustion.

Local analysis of the structure of the partially premixed flame shows deviations from the flamelet behavior. Two specific effects were identified: (1) the varying mixture fraction Z makes a flamelet analysis more delicate and (2) the interaction between rich and lean flame portions alter the local flame structure. This has strong implications for partially premixed combustion modelling, and is the subject of undergoing work in our group.

Acknowledgments

The authors gratefully acknowledge Dr. H. Pitsch for gently providing the iso–octane chemical kinetics scheme. We also acknowledge the "Institut du Développement et des Resources en Informatique Scientifique", IDRIS, for providing computing time.

References

[1] Y. Takagi. *27th Symposium (Int.) on Combustion*, 1998.

[2] F.Q. Zhao, M.C. Lai, and D.L. Harrington. *Prog. Energy Combust. Sci.*, 25:437–562, 1999.

[3] R.B. Krieger, R.M. Siebert, J.A. Pinson, N.E. Gallopoulos, D.L. Hilden, D.R. Monroe, R.B. Rask, A.S.P Solomon, and P. Zima. *SAE paper no. 972683*, 1997.

[4] A.H. Lefebvre. Gas Turbine Combustion. 2nd edition, Taylor & Francis, 1998.

[5] J. Zhou, K. Nishida, T. Yoshikazi, and H. Hiroyasu. *SAE paper no. 982563*, 1998.

[6] T. Poinsot, D. Veynante, A. Trouvé, and G. Ruetsch. *Proc. of the CTR Summer Program 1996*, 1996.

[7] J. Hélie and A. Trouvé. *27th Symposium (Int.) on Combustion*, 1998.

[8] D. Haworth, R. Blint, B. Cuenot, and T. Poinsot. *Combustion and Flame*, 121:395–417, 2000.

[9] C. Jiménez, B. Cuenot, T. Poinsot, and D. Haworth. *Combustion and Flame*, in press, 2001.

[10] M. Baum, T Poinsot, D. Haworth, and N. Darabiha. *Journal of Fluid Mechanics*, 281:1–32, 1994.

[11] S.K. Lele. *Journal of Computational Physics*, 103:16–42, 1992.

[12] H. Pitsch, N. Peters, and K. Seshadra. In *26th Symposium (Int.) on Combustion, The Combustion Institute, Pittsburgh*, page 763, 1996.

[13] R.J. Kee, J. A. Miller, and T.H. Jefferson. *SANDIA Tech, Report:SAND 83-8003*, 1980.

[14] R.J. Kee, J. Warnatz, and J. A. Miller. *SANDIA Tech, Report:SAND 83 -8209*, 1983.

[15] D. Haworth and T. Poinsot. *Journal of Fluid Mechanics*, 244:405–436, 1992.

List of Tables

List of Figures

Case	ϕ_{min}	ϕ_{max}	$\langle\phi\rangle$	$\langle\phi'^2\rangle$	$l_{\phi 0}/L_y$
H	.6	.6	.6	0	∞
NH1	.03	2.06	.6	.45	1
NH4	.03	2.06	.6	.45	1/4
$L_{x,y}$	$n_{x,y}$	τ_{T0}/τ_f	u'_{T0}/s_l^0	l_{T0}/δ_l^0	Re_{T0}
3 mm	451	.1	14.	1.35	100

Table 1: Equivalence ratio distributions and parameters relating turbulent characteristics to flame characteristics.

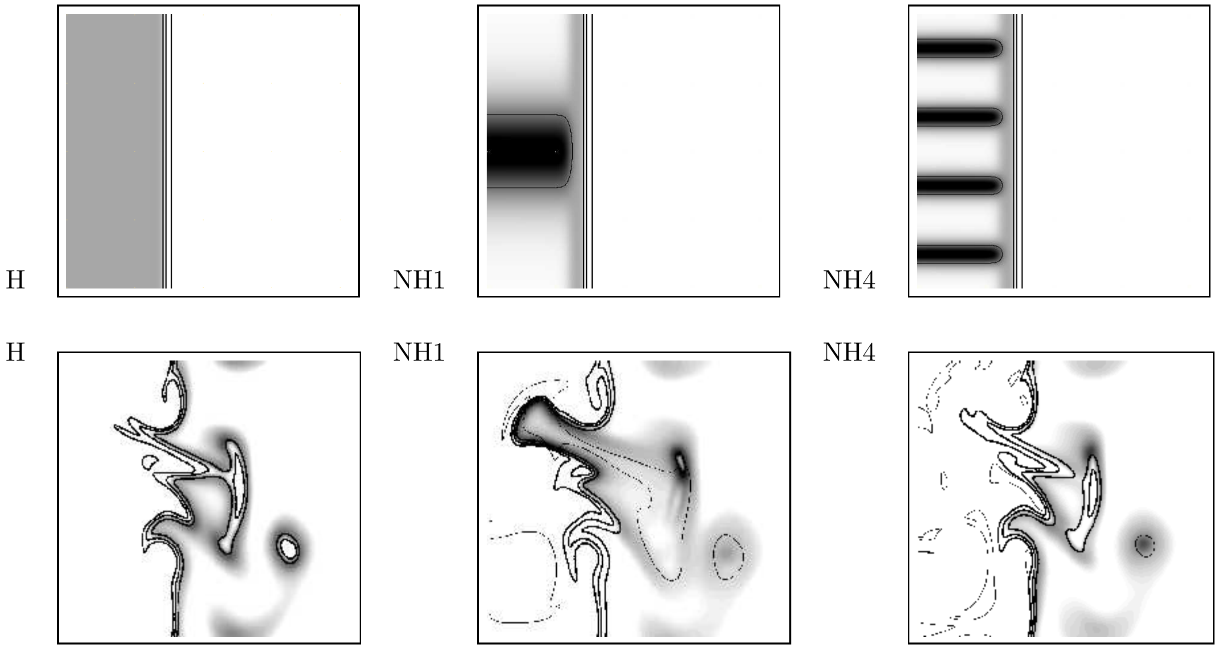

Figure 1: Top: Initial fuel mass fraction distribution in simulations H, NH1 and NH4. Bottom: heat release rate at time $t/\tau_f = 4$; the thick lines represent progress variable isocontours and the thin black line the stoichiometric line.

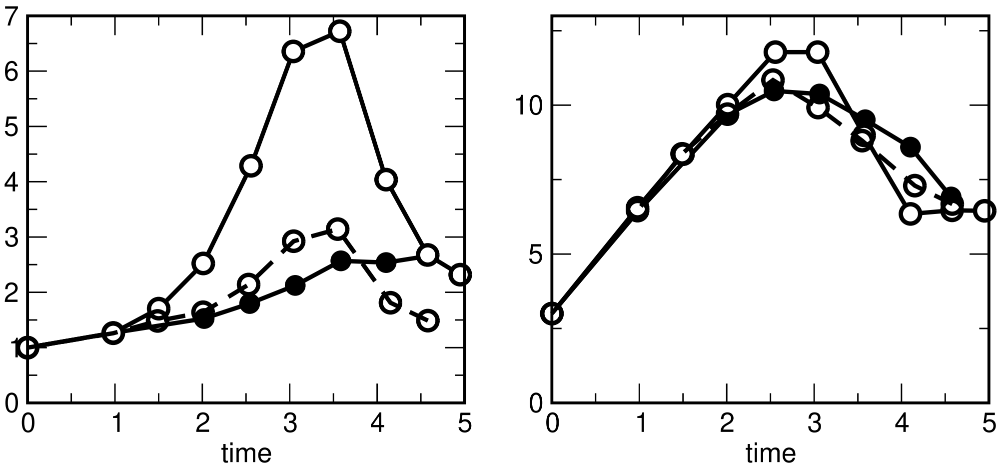

Figure 2: Time evolution of global heat release (Left: Q_{DNS}, normalized) and flame length (Right: Σ, mm) for flames H (–•–), NH1 (–∘–), and NH4 (- -∘ - -). Values of (Q_{DNS}) are normalized by the global heat release of a planar laminar flame with $\phi = .6$.

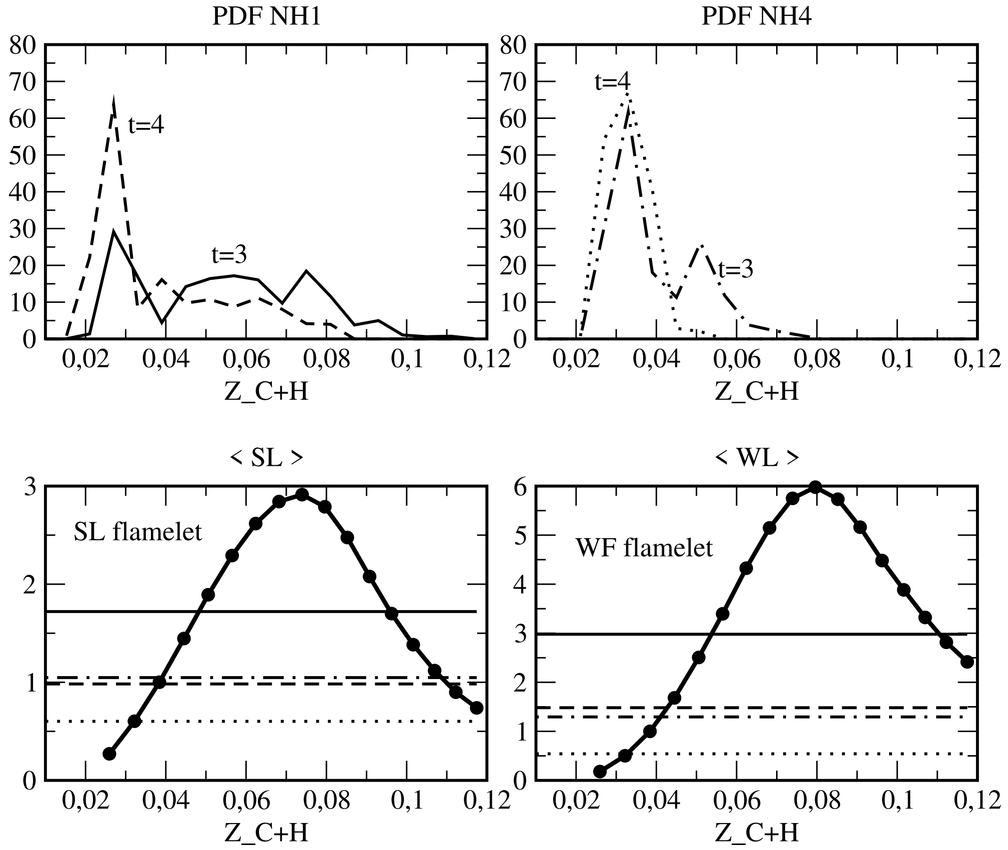

Figure 3: Top: PDFs of the Z distribution: — NH1, $t/\tau_f = 3$; - - - NH1, $t/\tau_f = 4$; - . . - NH4, $t/\tau_f = 3$; . . . NH4, $t/\tau_f = 4$. Bottom, left: $S_L(Z)$ obtained from the flamelet library normalized by its value at $< Z >= 0.37$ (–•–) and $< S_L(Z) >_\Sigma$ computed from the PDFs above (— NH1, $t/\tau_f = 3$; - - - NH1, $t/\tau_f = 4$; - . . - NH4, $t/\tau_f = 3$; . . . NH4, $t/\tau_f = 4$). Bottom, right: $W_L^F(Z)$ obtained from the flamelet library normalized by its value at $< Z >= 0.37$ (–•–) and $< W_L^F(Z) >_\Sigma$ computed from the PDFs above (— NH1, $t/\tau_f = 3$; - - - NH1, $t/\tau_f = 4$; - . . - NH4, $t/\tau_f = 3$; . . . NH4, $t/\tau_f = 4$)

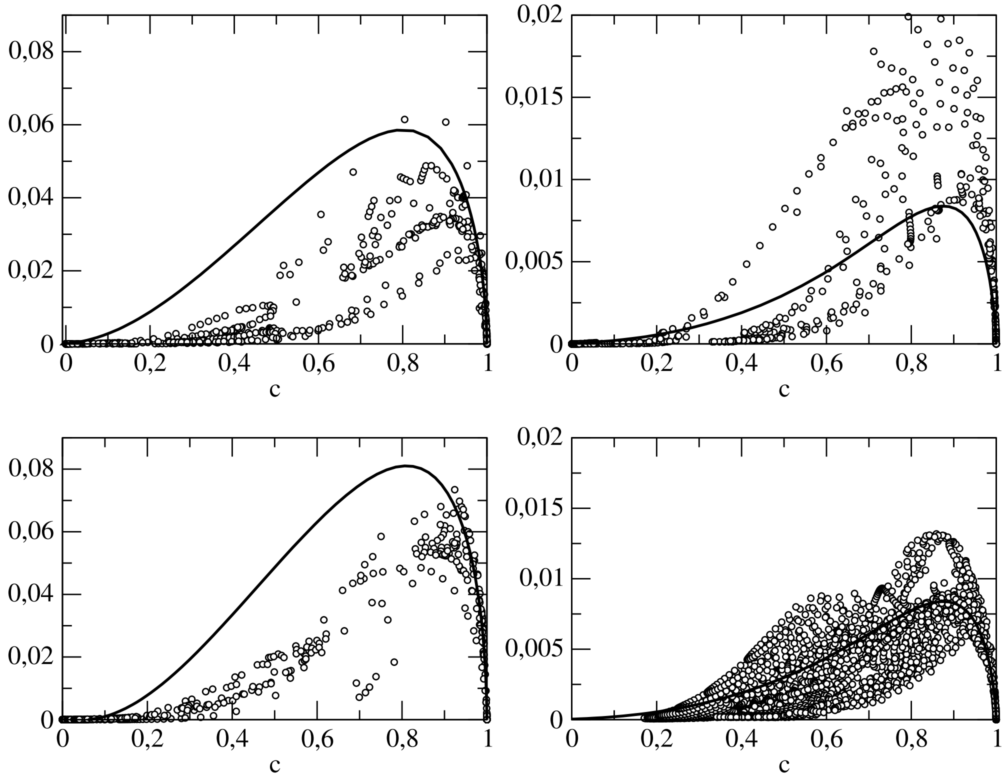

Figure 4: Comparison of laminar flamelet values (lines) and DNS values (scatter points) of the reaction rate $\dot{\omega}^F$ at $t/\tau_f = 3$ for cases H and NH1. From top to bottom and left to right: case NH1, $Z = .062$ ($\phi = 1$) ; case NH1, $Z = .0372$ ($\phi = .6$) ; case NH1, $Z = .0744$ ($\phi = 1.2$) and case H, $Z = .0372$ ($\phi = .6$)

.